Simple Driven Maps As Sensitive Devices

Changsong Zhou[1] and C.-H. Lai[1,2]
[1]Department of Computational Science
and [2]Department of Physics
National University of Singapore, Singapore 119260

Abstract

Sensitive dependence of nonlinear systems on initial conditions or parameters can be useful in applications. We propose in this paper that bubbling behavior in simple driven symmetrical maps may be used as a working principle of sensitive devices. The system is stable when there is no input and displays bursting behavior when there is small input. The symmetrical property of the bursting pattern is very sensitive to the bias of the noisy inputs, which makes the system promising for detecting weak signals among noisy environment.
PACS number(s): 05.45.+b;

A common property of many nonlinear systems is their sensitive dependence on initial conditions or parameters. This effect can be useful in applications. For example, the sensitivity of a chaotic system can be used to control its state to unstable periodic orbits embedded in it [1], in targeting the state of the system to desired points in the state space[2], to control the system to follow a desired goal dynamics in order to synchronize with another system[3] or to allow a message being encoded in a chaotic series for the purpose of secure communication[4], only by small modifications of the parameters or state of the chaotic system. The capability of achieving quite different behavior by applying only small perturbations improves greatly the flexibility of a system to be used in various applications.

By definition, sensitivity is referred to as the growth of small perturbations to the system. So, naively, sensitivity of nonlinear systems can be used to design sensor devices. Many systems possess a period-doubling bifurcation when some parameter is varied. Near the onset of a period-doubling bifurcation, any dynamical system can be used to amplify perturbations near half the fundamental frequency[5]. One disadvantage associated with the application of such parameter sensitivity for sensor device purpose is that the control parameter of the system must be located extremely close to the critical value of the bifurcation.

Recently, Böhme and Schwarz proposed to use two identical chaotic systems to construct sensitive devices[6]. In particular, they employed the following symmetrically coupled chaotic systems

$$\dot{x} = f(x) - k(x-y) + s_{in}, \tag{1}$$
$$\dot{y} = f(y) + k(x-y) - s_{in}, \tag{2}$$

named chaotic bridge as a sensor device. s_{in} represents a constant input to be sensed. The coupling gain k is chosen near the threshold k_c of synchronization, so that for $s_{in} = 0$, the coupled systems are in synchronization state, and the output $s_{out} = ||x - y|| = 0$; while for $s_{in} \neq 0$, the symmetry of the chaotic bridge is broken, and it may have a large output at some moment. Since the synchronization manifold is transversely stable for $s_{in} = 0$, there must exist local instabilities in the system in order to obtain amplification of small perturbations. As pointed out by the authors in [6], in the neighborhood of the boundary k_c of synchronization, one can expect the highest sensitivity of the system.

We would like to highlight the connection of the working principle of the above device to the phenomenon of *attractor bubbling* studied recently[7-10]. When k is just beyond the threshold k_c, the synchronization manifold is transversely stable. However, there still exist some invariant sets, such as the unstable periodic orbits embedded in the synchronization manifold, which are transversely unstable. As a consequence, small perturbations in the systems which destroy its synchronization manifold will result in large intermittent bursts from the synchronization manifold, no matter how small the perturbations are[8]. This is the origin of the sensitivity of the above system. The difficulties of application of the system for sensor devices lie in practical implementations. Just like additive perturbations, any parameter mismatches between the systems can also lead to intermittent bursts. Parameter mismatches are inevitable in experiment implementations. This is the reason that intermittent desynchronization was observed beyond the threshold of synchronization in many experiments of

synchronization between well matched electrical circuits[7-10]. This effect imposes great difficulties in the experimental implementation of the above sensor devices, because inevitable parameter mismatches lead to large output even for $s_{in} = 0$. The above devices can work only if the two systems are *ideally identical*, which is extremely difficult to realize. On the other hand, small external noise can also result in large bursts when $S_{in} = 0$, which makes it very difficult to tell a signal from noise which is always present in the practical environment.

To avoid the above difficulties, we propose in the following to use simple driven systems as sensor devices.

Attractor bubbling and on-off intermittency[11,12] are common behaviors that occur in coupled nonlinear systems which possess an invariant manifold. They can be achieved in very simple parametrically driven one-dimensional maps[12]

$$y_{n+1} = z_n f(y_n), \tag{3}$$

where $f(0) = 0, \partial f(y)/\partial y|_0 \neq 0$, and $z_n = ax_n > 0$ is random or chaotic driving signal with density function ρ_z and a is a parameter. For the purpose of the application of the systems as sensitive devices, we require the maps to have odd symmetry, i.e. $f(-y) = -f(y)$.

The stability of the invariant manifold $y = 0$ is governed by the linear equation

$$y_{n+1} = z_n y_n, \tag{4}$$

which describes the evolution of small perturbations transverse to the invariant line $y = 0$. Here $\partial f(y)/\partial y|_0$ is absorbed into the parameter a. The transverse Lyapunov exponent λ of the invariant manifold defined as

$$\lambda = \lim_{N\to\infty} \frac{1}{N} \sum_{n=1}^{N} \ln z_n =< \ln z > \tag{5}$$

determines the stability of the invariant manifold. The critical point a_c at which $\lambda = 0$ is the onset point of on-off intermittency[12]. For z_n being a uniform random driving signal on $(0, a)$, $\rho_z = 1/a$, and $< \ln z >= \ln a - 1 = 0$ gives $a_c = e$. Just above the onset point, $a \geq a_c$, the random driven system displays universal features of on-off intermittency behavior, which are unaffected by the form of the confining nonlinearity[12]. The nonlinearity of the system serves to bound or reject the dynamics back towards small values of y after bursts. For a below a_c, the invariant manifold $y = 0$ is stable, but the stability is quite weak if a is near a_c. Attractor bubbling occurs in the system when there are inputs of perturbations such as noise.

For a sensitive device, it should be stable when there is no input, and is expected to produce large outputs when there are small perturbations. In this paper, we are not considering the on-off intermittency behavior with $a \geq a_c$. For the purpose of sensor purpose, we employ the bubbling behavior with $a < a_c$. The sensor system reads

$$y_{n+1} = z_n f(y_n) + s_{in}, \tag{6}$$

and $s_{out} = y$. When there is no input, i.e. $s_{in} = 0$, $y = 0$ is a stable solution, and the output $s_{out} = 0$. Since the critical parameter a_c and the evolution of small perturbations

are independent of the form of the nonlinearity, one can choose a map which is simple for implementation. For example, we employ a piecewise linear map

$$f(y) = \begin{cases} \frac{c_1}{c_2}(-c_1 - c_2 - y), & y < -c_1, \\ y, & |y| \le c_1, \\ \frac{c_1}{c_2}(c_1 + c_2 - y), & y > c_1, \end{cases} \tag{7}$$

where c_1 and c_2 are two parameters, as shown in Fig. 1.

If there is no input, $s_{in} = 0$, staring from a small initial condition $y_0 = p$, we have $y_n = z_{n-1}z_{n-2}\cdots z_0 p = k_n p$. The average order of the factor k_n, which can be defined as $< \ln k_n >$, decreases linearly with n as

$$< \ln k_n >= n < \ln z >= n(\ln a - 1). \tag{8}$$

Now, suppose there is a small constant input $s_{in} = p$, starting from $y_0 = 0$, the evolution of the output reads

$$\begin{array}{c} y_1 = (z_0 + 1)p = k_1 p, \\ y_2 = (z_1 z_0 + z_1 + 1)p = k_2 p, \\ \cdots \\ y_n = (z_{n-1}\cdots z_0 + \cdots + z_{n-2}z_{n-1} + z_{n-1} + 1)p = k_n p, \end{array} \tag{9}$$

if $\max(|y_n|) = |p|(1+a+\cdots a^n) = |p|\frac{a^{n+1}-1}{a-1} \le c_1$, or, $n \le n_c = \mathrm{int}[\ln(c_1(a-1)/|p|+1)/\ln a]-1$, where int$[x]$ is the interger part of a real number x. The average order of k_n, $< \ln k_n >$, cannot be obtained analytically as that for $s_{in} = 0$ in Eq. 8. A numerical estimation of $< \ln k_n >$ is carried out with 10^6 samples of k_n. Unlike the case $s_{in} = 0$, it is an increasing function of n, as shown in Fig. 2.

When $n > n_c$, y_n has nonvanishing probability to exceed $y_n > c_1$. Following Böhme and Schwarz, a measure s for the sensitivity of the system to constant input can be defined as

$$s = \frac{\max\limits_n |y_n|}{|s_{in}|}. \tag{10}$$

Since $\max(k_n) = \frac{a^{n+1}-1}{a-1}$ increases exponentially with n, an infinitely small input value can create a finite output. The largest output $\max\limits_n |y_n| = ac_1$ is due to the confinement of the nonlinearity of the map. The sensitivity s of the system thus goes to infinity and is referred to as *supersensitivity*[6].

An important question concerning the system is the time needed for small input to produce a large output. We examine the time N for a small input p to produce for the first time an output $s_{out} \ge c_1$. The distribution $P(N)$ of N is the following probability

$$P(N) = \mathrm{Prob}(\bigcap_{i=1}^{N-1} y_i < c_1 \bigcap y_N \ge c_1). \tag{11}$$

By defining the event $E_N = \bigcap_{i=1}^{N} y_i < c_1$ and the corresponding probability $\Lambda_N = \mathrm{Prob}(E_N)$, it follows that

$$P(N) = \Lambda_N - \Lambda_{N-1},$$

which is a function of both a and p. In principle, Λ_N can be evaluated by the joint density $\Phi(K)$ of $k_1, k_2, \cdots, k_N$, namely,

$$\Phi(K) = \frac{\rho(z_0)\rho(z_1)\cdots\rho(z_{N-1})}{|J|} = \frac{\rho(k_1-1)\rho(\frac{k_2-1}{k_1})\cdots\rho(\frac{k_N-1}{k_{N-1}})}{k_1 k_2 \cdots k_{N-1}},$$

where J is the Jacobian of the transformation between k_i's and z_i's defined in Eq. (9). Specifically, one has

$$\Lambda_N = \int_1^b dk_N \int_{(k_N-1)/a}^b \rho(\frac{k_N-1}{k_{N-1}})\frac{dk_{N-1}}{k_{N-1}} \cdots \int_{(k_{i+1}-1)/a}^b \rho(\frac{k_{i+1}-1}{k_i})\frac{dk_i}{k_i}\cdots$$

$$\times \int_{(k_2-1)/a}^b \rho(\frac{k_2-1}{k_1})\rho(k_1-1)\frac{dk_1}{k_1}$$

where $b = c_1/p$ if $i > n_c$ and $b = \frac{a^{i+1}-1}{a-1}$ if $i \leq n_c$. However, to the best of our knowledge, a closed-form solution of the above integral for any N is not available.

In the following, we are going to carry out some simulations. We specify $c_1 = 1$ and $c_2 = 2$ in these simulations. In Fig. 3, as an example, the output sequence is shown for $s_{in} = 1.0 \times 10^{-4}$ at $a = 2.6$. The dashed lines indicate the switch on and off of the constant input. The output in the presence of input is a intermittent process, similar to the result of the chaotic bridge in [6].

In the next simulation, we estimate $P(N)$ for different values of a and p, as shown in Fig. 4. It is seen that the distributions peak at rather small N values, and after the peak, they decrease exponentially. The average time $< N >$ for first putting out $y_N \geq c_1$ is also evaluated as a function of a and p in Fig. 5(a) and (b), respectively. So, on average, the closer the a to a_c and the larger the input p, the quicker the system reaches a large output.

The simulation results show that this system may be used as a detector for weak signal. However, the above discussion is only valid in a noise-free environment. In the practical application of the system as a detector, external noise is unavoidable. The system now reads

$$y_{n+1} = z_n f(y_n) + s_{in} + e_n, \tag{12}$$

where e_n denotes external noise. It is plausible to assume that e_n has vanishing mean value and a Gaussian distribution $\sigma N(0,1)$, with a standard deviation σ. The behavior of the system in the presence of noise is quite different from the noise-free case, because bubbling occurs even without a signal s_{in}. Very small external noise can also lead to large output of the system, as illustrated in Fig. 6 (a) with $a = 2.6$ and $\sigma = 1 \times 10^{-4}$. In this system with $a < a_c$, bursting behavior always means that there are some inputs to the system, and the largest output will be independent of the inputs. The problem now becomes whether we can distinguish that the input is a meanful signal or just noise, and moreover whether we can

detect any significant signal among the white noise environment. As will be shown in the following, this system is quite promising for this task, because the symmetrical property of the bursting behavior is very sensitive to the bias of the inputs.

This sensitivity is due to the odd symmetry of the map. An inspection of Fig. 6(a) reveals that the number of large bursts to positive and negative values is quite symmetric for inputs of white noise. When a small positive constant input $s_{in} = p = 0.3 \times 10^{-4}$ is present along with the noise, the symmetry is clearly broken, as seen in Fig. 6(b). Note that the constant input p is much smaller than the noise level σ in this example. This result indicates that the symmetry of burst is quite sensitive to the bias of the total inputs $s_{in} + e_n$ of the system. To characterize the symmetry breaking property quantitatively, we introduce the degree of asymmetry D_{asy} as

$$D_{asy} = \frac{N_+ - N_-}{N_+ + N_-}, \tag{13}$$

where N_+ (N_-) is the number of large burst ($|y| \geq 1$) to positive (negative) values during a period of observation time T. Because of the symmetry of the map and that of the white noise, one can expect that $D_{asy} \approx 0$ for white noise inputs. For positive (negative) constant inputs in the noise-free case, it is clear that $D_{asy} = 1(-1)$.

A comparison between Fig. 6(a) and (b) also shows that large bursts occur more frequently when constant input is present with the noise. We define the bursting frequency F as

$$F = \frac{N_+ + N_-}{T}. \tag{14}$$

We expect that F increases with larger constant input p and larger noise level σ.

A measure of the significance of a constant signal among the noise can be the "signal to noise ratio" $R = p/\sigma$. In the following, simulations are carried out to examine the dependence of D_{asy} and F on R for different noise level σ and system parameter a. The results shown in Fig. 7 are obtained with $T = 2 \times 10^6$. The result of D_{asy} is very interesting: as a function of R, D_{asy} is independent of the noise level σ and is not sensitive to parameter a. Whether a constant signal embedded in the noise environment can be detected depends only on its significance with respect to the noise level. However, a and σ have effect on the bursting frequency F, as seen from Fig. 7(b). A combination of Fig. 7(a) and (b) makes it possible to determine the noise level and R, and thus to estimate the amplitude of the constant signal in a observation.

To get a good estimation of D_{asy} and F, T should be large enough. In practice, one may not expect a signal that stays constant for so long a time. The term *constant signal* is a concept relative to the time scale of the detector, and the time scale can be controlled in the implementation. In numerical experiment of this dimensionless system, we can simulate a shorter signal (or a "slower" detector) with smaller T, e.g., $T = 2000$. In this case, D_{asy} has large fluctuations, as shown in Fig. 8(a) where D_{asy} of 20 realizations of the driving z_n and white noise e_n of the system are plotted for each R value. When R is getting larger, more points coincide at $D_{asy} = 1$. A good way to examine the fluctuation behavior is to construct a histogram of D_{asy}, as shown in Fig. 8(b) for $a = 2.6, \sigma = 10^{-4}$. The results show that even for quite short signal and low R value, D_{asy} has very high probability near $D_s = 1$. An

implication of the results is that several detectors can be used at the same time to detect and confirm a short and weak signal embedded in white noise.

As an example of a little more realistic input signal, we present the response of the system to the noisy input $A\sin(0.003n)+e_n$, where the noise level is $\sigma = 1\times 10^{-4}$ and the amplitude of the sine wave is $A = 0.3 \times 10^{-4}$. Both the total input and the output of the system are displayed in Fig. 9. The bursting feature reflects the weak wave among the noise quite clearly.

In summary, we have shown that a kind of very simple driven symmetrical maps below the onset point of on-off intermittency have two distinguishing features of (i) being stable at the invariant state $y = 0$ and (ii) being sensitive to small input. In practice, the environment cannot be noise-free, and the systems exhibit bubbling behavior in the presence of noise. Another interesting and useful property of the systems is that the bursting pattern is symmetrical for white noise input, and the symmetry is broken when there is signal among the noise environment. The significance of the signal is manifested by the degree of asymmetry in the bursting pattern. These features make them promising candidates for designing sensitive devices.

Although our study is based on numerical simulations of a mapping model, it should be noted that system response to small inputs is governed by its linearized equation, and the nonlinearity only serves to keep the system bounded. Many long time properties shown above thus are universal in a class of driven systems possessing odd symmetry. The following can be advantages for such systems when considering applications in sensitive devices:

1) The sensitivity is maintained in a large range of parameter below the critical point. This avoids the difficulty of locating parameter in a very small neighborhood of a bifurcation point in a period-doubling system.

2) The sensitivity of the system is, in principle, infinite. In a noise-free environment, an infinitesimal input signal can produce a finite output. When noise is present, weak signal can also be manifested by the asymmetry in the bursting pattern. The degree of asymmetry depends on the significance of the signal with respect to the noise. The sensitive behavior is universal for different forms of nonlinearity of the systems, as well as for different form of driving signals. This is very useful because one can thus choose a system that is simple and easy to implement in practice.

It could be meaningful to consider implementation of such simple systems and explore their application in small signal detection. Since in applications, pivotal role is played by the symmetry properties of the system, one should take care to maintain such properties. In order to avoid perturbations which may make the system appreciably asymmetric, one should avoid using different parameters for the two symmetrical parts of the systems. Also, one should note that it takes longer for the system to produce static output states for lower level of inputs. There seems to be a frequency cutoff associated with the input levels and the relaxation time of the systems. Above the cutoff, the small signal in the noise can no longer be manifested by clear asymmetry in the bursting pattern. Such limits should be taken into consideration in applications.

Acknowledgements:

This work was supported in part by research grant RP960689 at the National University of Singapore. CZ was supported by NSTB.

References

1. E. Ott, C. Grebogi, and J. Yorke, Phys. Rev. Lett. **64**, 1196(1990).

2. T. Shinbrot, E. Ott, C. Grebogi, and J. Yorke, Phys. Rev. Lett. **65**, 3215(1990); T. Shinbrot, *et al*, Phys. Rev. Lett. **68**, 2863 (1992).

3. Y. C. Lai, C. Grebogi, Phys. Rev. E **47**, 2357 (1993).

4. S. Hayes, C. Grebogi, and E. Ott, Phys. Rev. Lett. **70**, 3031(1993); S. Hayes, C. Grebogi, E. Ott, and A. Mark, Phys. Rev. Lett. **73**, 1781(1994); E. M. Bollt and M. Dolnik, Phys. Rev. E **55**, 6404 (1997).

5. K. Wiesenfeld and B. McNamara, Phys. Rev. Lett. **55**, 13(1985).

6. F. Böhme and W. Schwarz, in *Nonlinear Dynamics of Electronic Systems*, eds by A.C. Davies and W. Schwarz (World Scientific, Singapore, 1994), pp 281.

7. P. Ashwin, J. Buescu, and I. Stewart, Phys. Lett. A **193**, 126(1994).

8. J. F. Heagy, T. L. Carroll, and L. M. Pecora, Phys. Rev. E **52**, R1253(1995).

9. D. J. Gauthier and J. C. Bienfang, Phys. Rev. Lett. **77**, 1751(1996).

10. S. C. Venkataramani, B. R. Hunt, E. Ott, D. J. Gauthier, and J. C. Bienfang, Phys. Rev. Lett. **77**, 5361(1996).

11. N. Platt, E. A. Spiegel, and C. Tresser, Phys. Rev. Lett. **70**, 279 (1993).

12. J. F. Heagy, N. Platt, and S. M. Hammel, Phys. Rev. E **49**, 1140 (1994).

Figure Captions

Fig. 1 The piecewise linear map $f(y)$. Here $c_1 = 1$ and $c_2 = 2$.

Fig. $2 < \ln k_n >$, the average order of k_n, as a function of n. It decreases linearly for the case without input (plot a) and increases for the case with input (plot b).

Fig. 3 An illustration of the output process of the sensitive system at $a = 2.6$. The constant input is $p = 10^{-4}$, and is switched on and off alternately for every 500 iterations, as shown by the dashed lines.

Fig. 4 Numerically evaluated distribution of N. The parameters of the plots are: (a) $a = 2.5, p = 10^{-3}$, (b) $a = 2.5, p = 10^{-4}$ and (c) $a = 2.6, p = 10^{-4}$.

Fig. 5 (a) Average value of N as a function of a with $p = 10^{-3}$, and (b) as a function of p with $a = 2.6$.

Fig. 6 (a) Output of the system when only white noise is present as input. (b) Output of the system when constant signal $p = 0.3\sigma$ is present along with the noise. The parameters are $a = 2.6, \sigma = 1 \times 10^{-4}$. Noting the change of symmetrical property of the bursting pattern of the system.

Fig. 7 (a) Degree of asymmetry D_{asy} as a function of "signal to noise ratio" R for different a and σ. (b) Bursting frequency F as a function of R for different a and σ. (b) shares the same legends of (a). The results are obtained from observation during a period of time $T = 2 \times 10^6$.

Fig. 8 (a) D_{asy} of short time observation, $T = 2000$. (b) Normalized histograms of D_{asy} for different R value. The histograms are constructed with 50000 observations for each R value. The parameters are $a = 2.6, \sigma = 1 \times 10^{-4}$.

Fig. 9 (a) A weak sine wave embedded in the noise. (b) The response of the detector to the inputs of (a).

Fig. 5

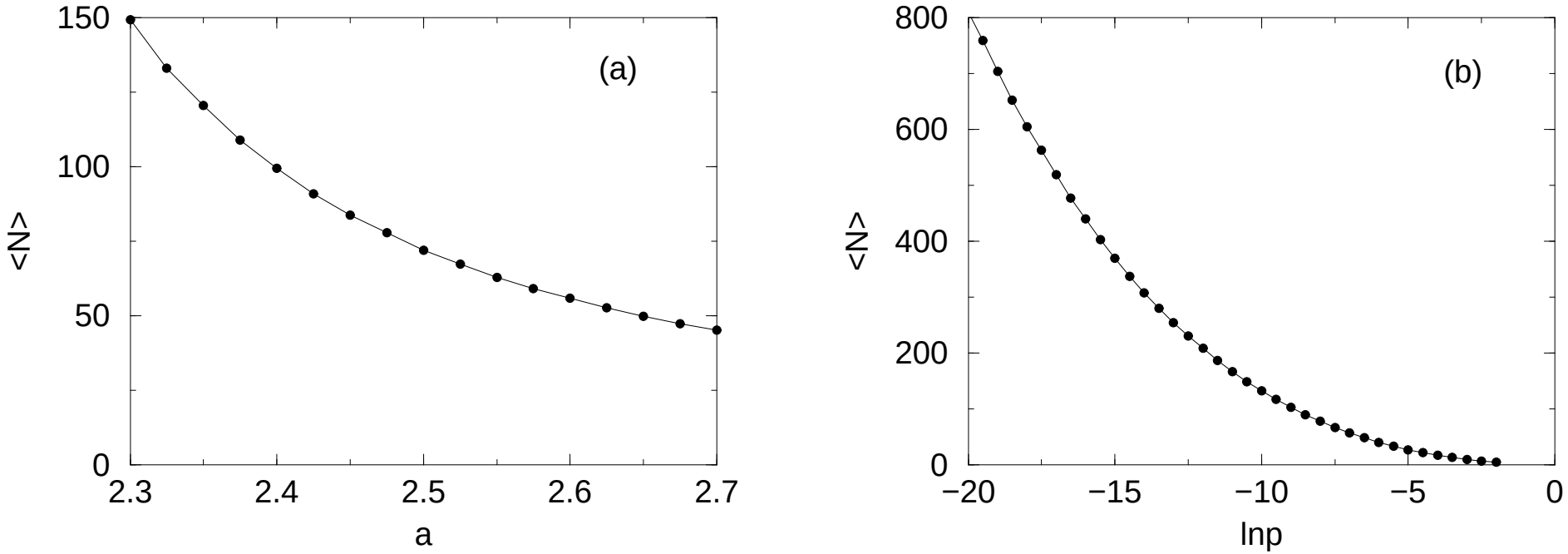

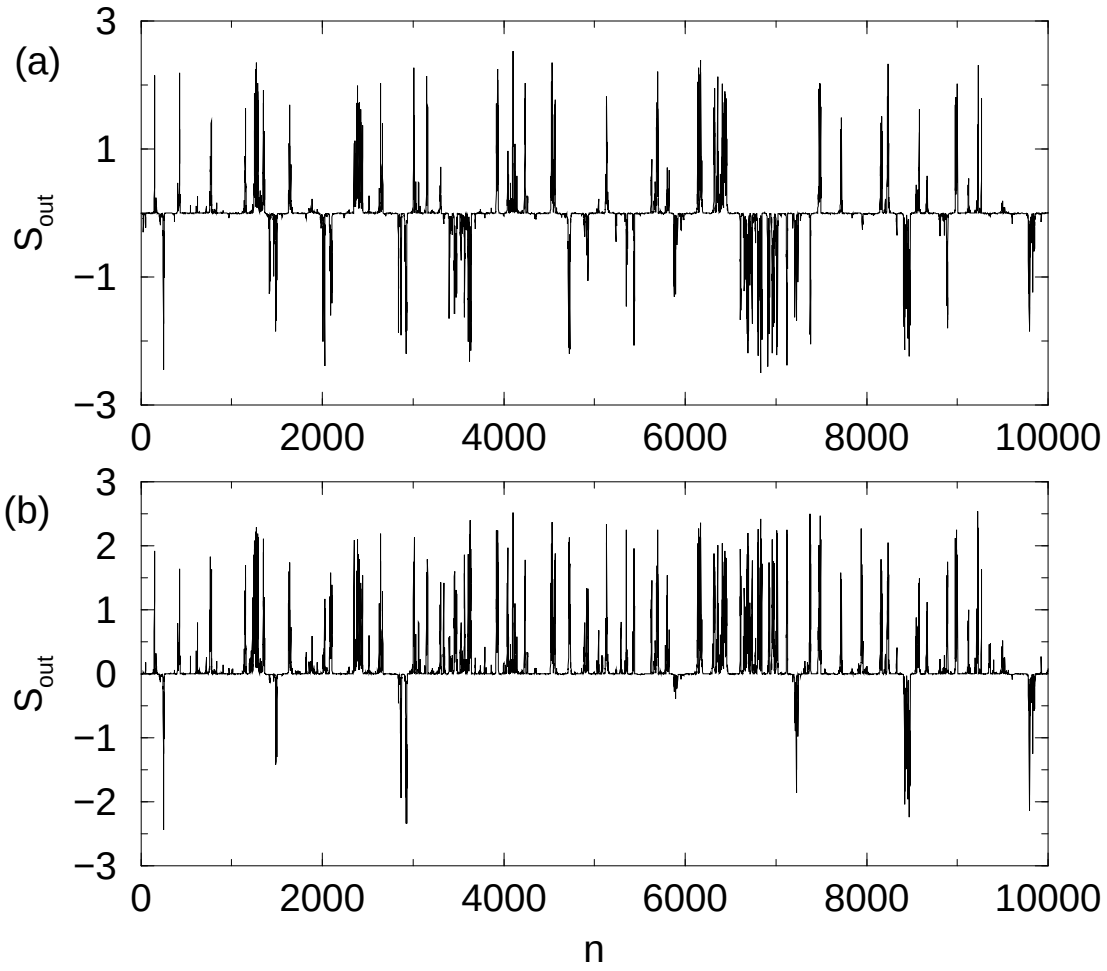

Fig6

Fig. 7

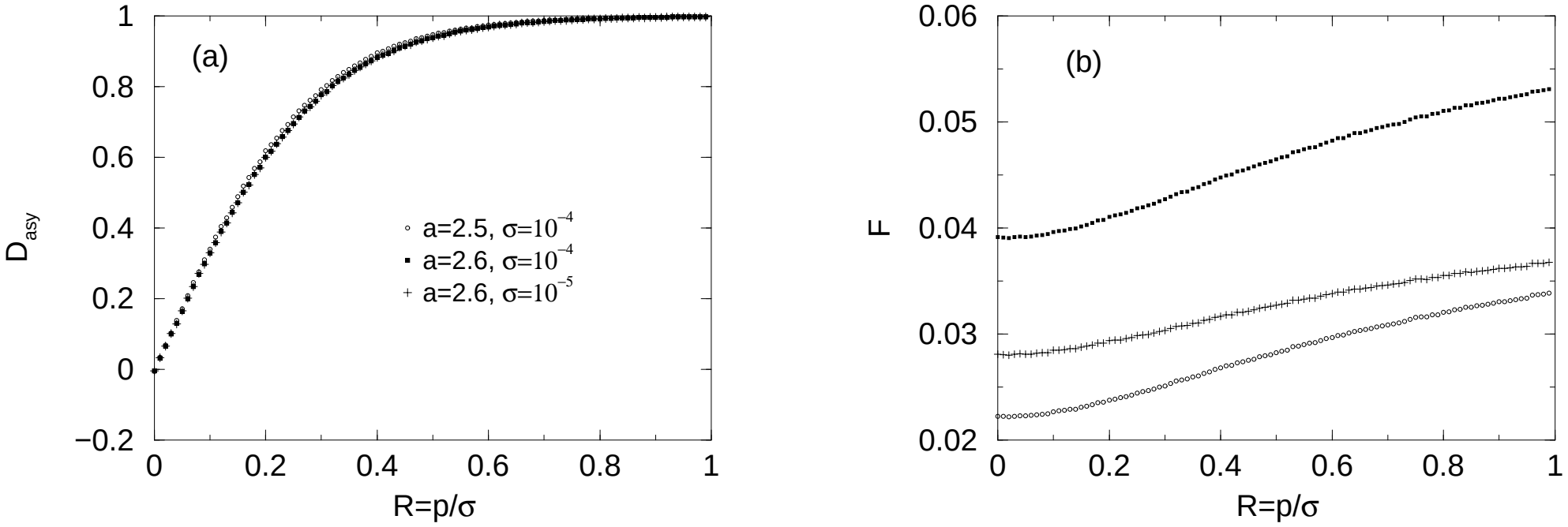
(a)
D_{asy}
R=p/σ
a=2.5, σ=10^-4
a=2.6, σ=10^-4
a=2.6, σ=10^-5
1
0.8
0.6
0.4
0.2
0
−0.2
0
0.2
0.4
0.6
0.8
1
(b)
F
R=p/σ
0.06
0.05
0.04
0.03
0.02
0
0.2
0.4
0.6
0.8
1

Fig. 8

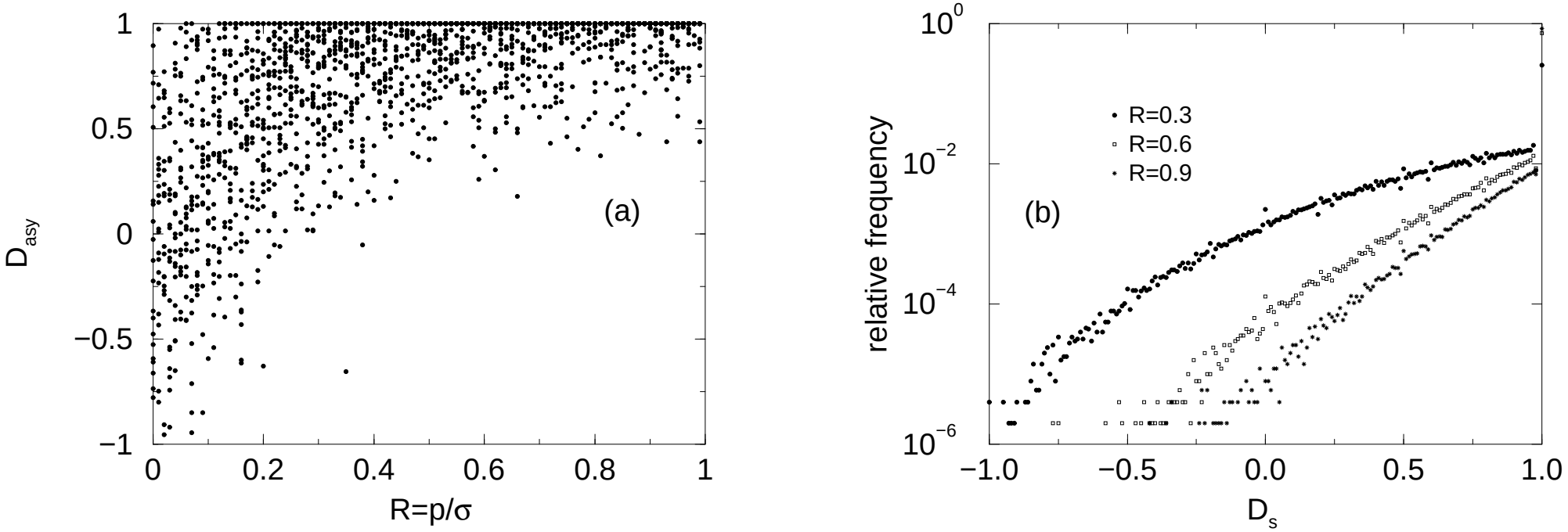
1
0.5
0
−0.5
−1
0
0.2
0.4
0.6
0.8
1
D_asy
R=p/σ
(a)
10^0
10^−2
10^−4
10^−6
relative frequency
R=0.3
R=0.6
R=0.9
(b)
−1.0
−0.5
0.0
0.5
1.0
D_s

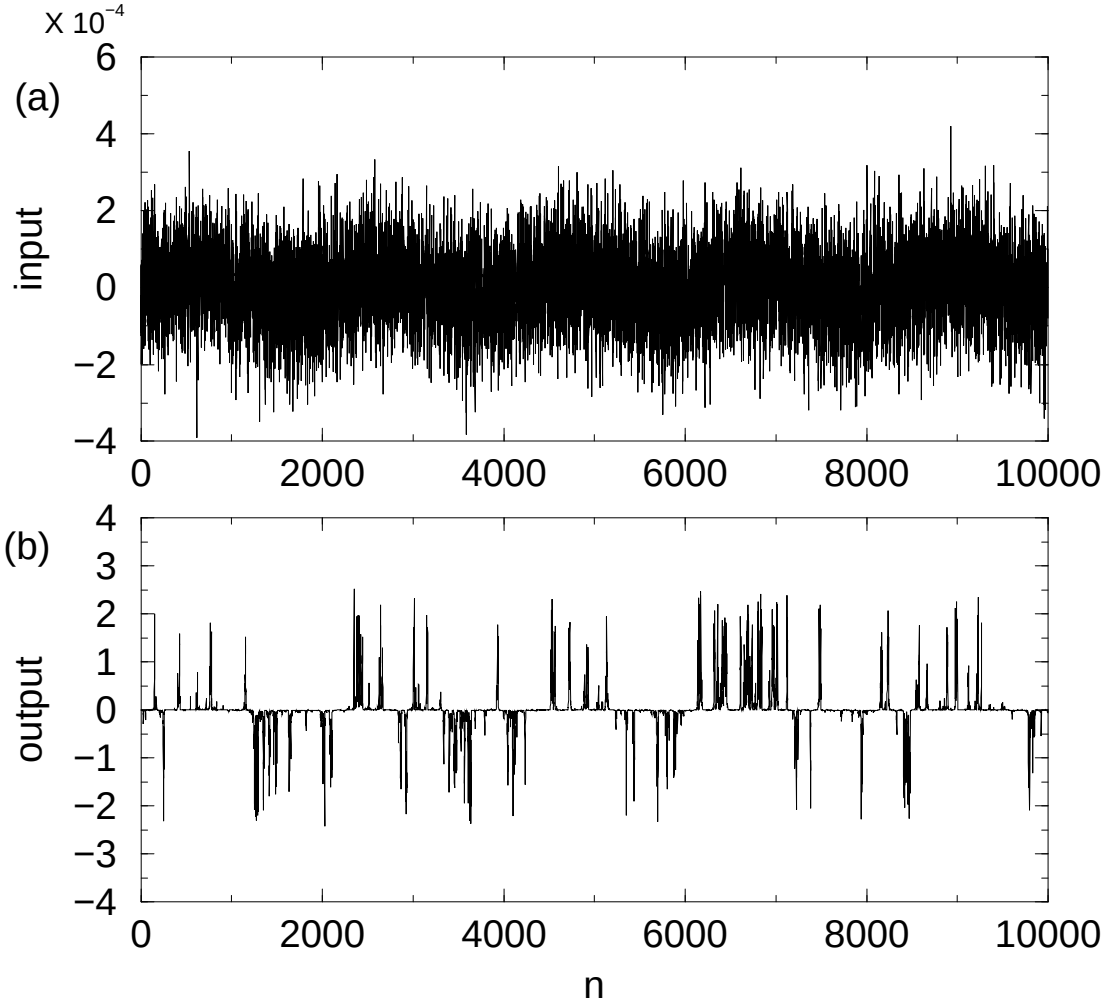
X 10^-4
(a)
input
6
4
2
0
−2
−4
0
2000
4000
6000
8000
10000
(b)
output
4
3
2
1
0
−1
−2
−3
−4
0
2000
4000
6000
8000
10000
n

Fig. 9

Fig. 1

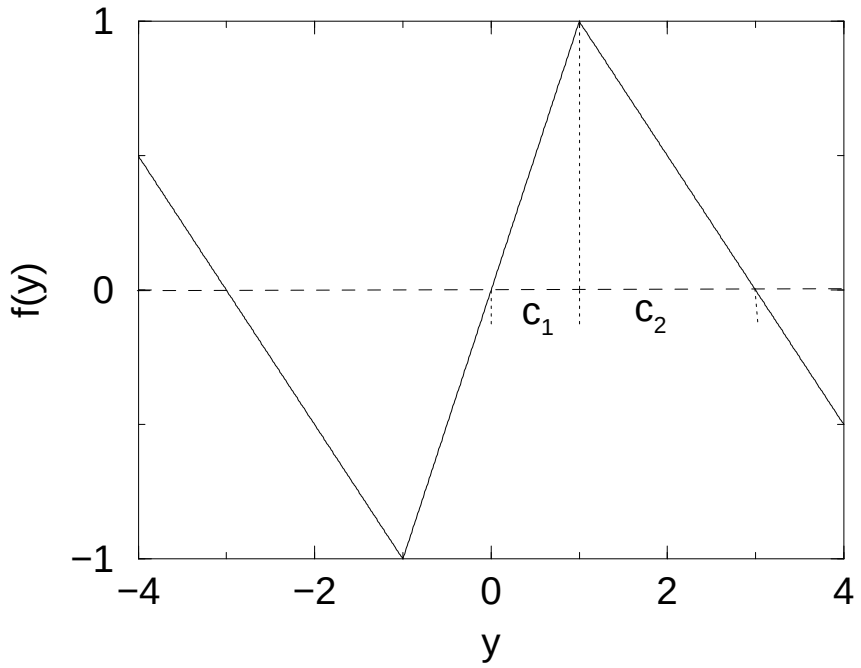

Fig. 2

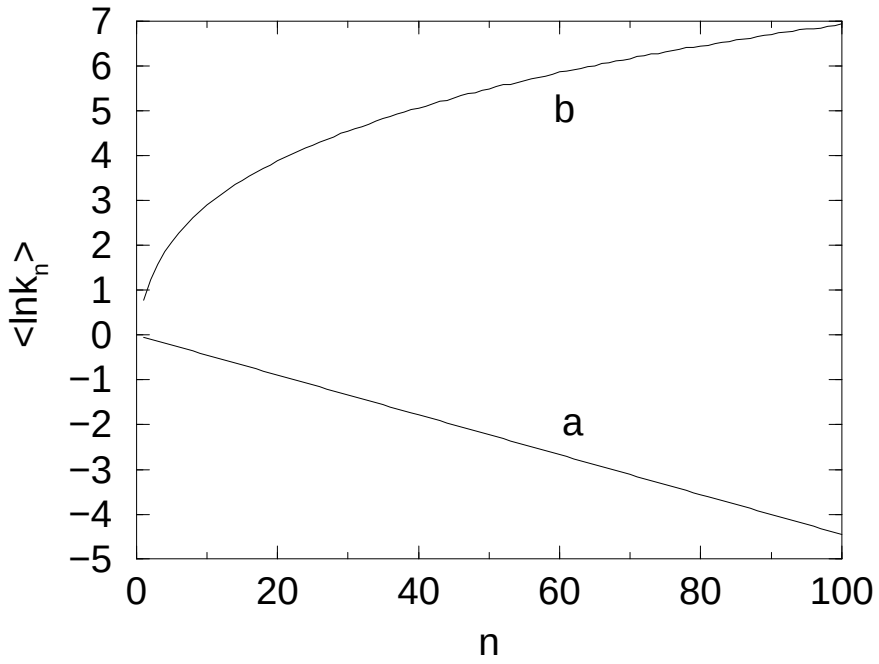

Fig. 3

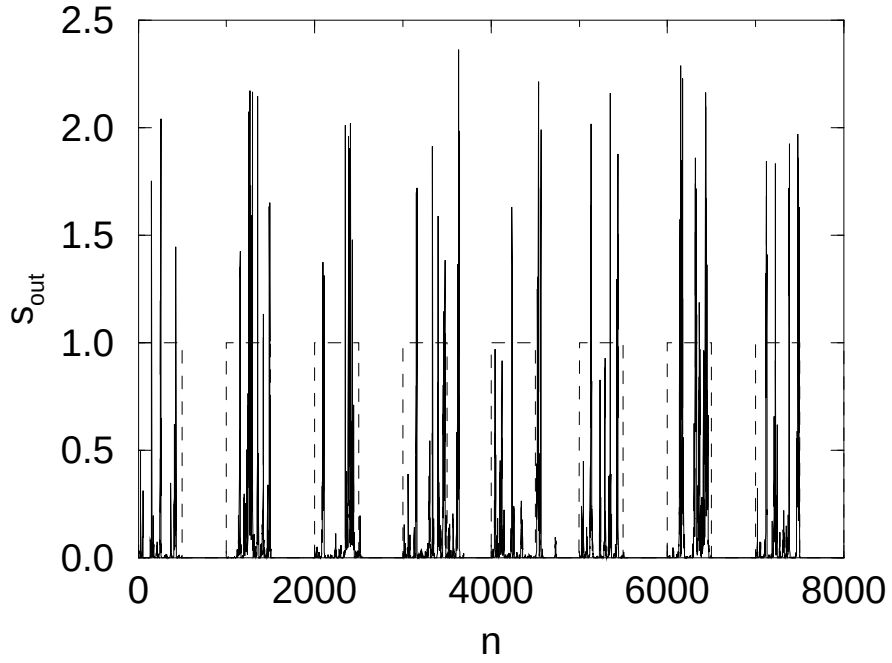
2.5
2.0
1.5
1.0
0.5
0.0
s_{out}
0
2000
4000
6000
8000
n

Fig. 4

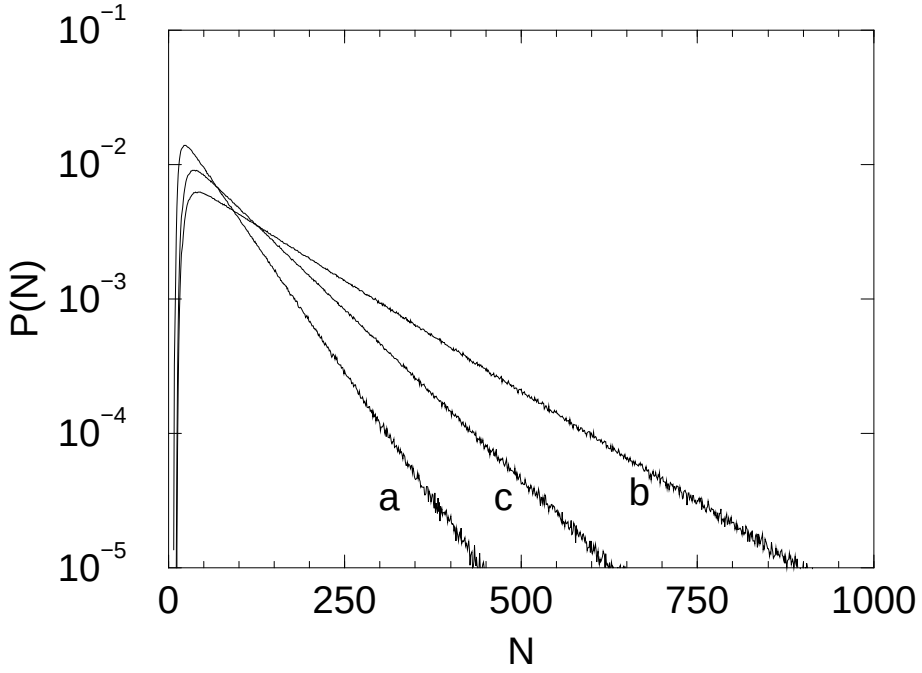
10^{-1}
10^{-2}
10^{-3}
10^{-4}
10^{-5}
P(N)
a
c
b
0
250
500
750
1000
N